Hydrolysis behavior of various crystalline celluloses treated by cellulase of Tricoderma viride

AUTHOR(S):

Abdullah, Rosnah; Saka, Shiro

Hydrolysis behavior of various crystalline celluloses treated by cellulase of *Tricoderma viride*

Rosnah Abdullah and Shiro Saka*

Department of Socio-Environmental Energy Science,
Graduate School of Energy Science, Kyoto University,
Yoshida-honmachi, Sakyo-ku 606-8501, Kyoto, Japan

*Shiro Saka
Tel/Fax: +81(0)75 753 4738
Email address: saka@energy.kyoto-u.ac.jp

Abstract

Cellobiose and glucose are valuable products that can be obtained from enzymatic hydrolysis of cellulose. This study discusses changes in the crystalline form of celluloses to enhance the production of sugars and examines the effect on structural properties during enzymatic hydrolysis. Various crystalline celluloses consisting of group I (cell I, cell III_I, cell IV_I) and group II (cell II, cell III_{II}, cell IV_{II}) of similar DPs were prepared as starting materials. The similar DP values allowed a more direct comparison of the hydrolysis yields. The outcomes were analyzed and evaluated based on the residues and supernatants obtained from the treatment. As a result: 1) action of the cellulase of *Trichoderma viride* decreased both DP and crystallinity, with greater changes in group II celluloses, 2) the polymorphic interconversion process that occurred for cell III_I, cell IV_I, cell III_{II} and cell IV_{II} during the treatment was independent of the enzymatic hydrolysis, thus, the hydrolysis behaviors depended on the starting material of the celluloses, and 3) higher sugar production was obtained from cell III_I and group II. Therefore, the hydrolysis behavior of the various crystalline celluloses depended on the particular polymorph of the starting material.

Keywords *Cellulose • Cellulase • Crystalline structure • Hydrolysis • Trichoderma viride*

Introduction

As cellulose is a main component of plant cell walls and the most abundant polymer in nature, its exploitation for biofuels, particularly bioethanol, has become a major research focus worldwide (O'sullivan 1997; Schacht et al. 2008). By the process of saccharification, glucose, cellobiose and other sugars can be obtained from cellulose. Those small sugars can be fermented to produce ethanol (Ward 2011). Thus, a conventional sequence that has been practised widely, is that to treat lignocelluloses with acid/alkali or sub/supercritical water, and/or later followed by enzymatic hydrolysis (Hsu 1996; Kumar et al. 2010).

Enzymatic hydrolysis of cellulose is a slow process and the extent of hydrolysis is influenced by structural properties such as crystallinity, surface area, DP, etc (Fan et al. 1980; Lee et al. 1983; Yoshida et al. 2008; Hall et al. 2010). Native cellulose is composed of β-D-glucopyranose units linked together in linear chains by β-1,4-glucosidic bonds, forming a crystalline material. Most practical cellulose samples appear to contain both crystalline and amorphous cellulose (Andersson et al. 2003; Igarashi et al. 2006). Completely disordered or amorphous cellulose could be hydrolyzed at a much faster rate, thus, knowledge of the initial degree of crystallinity is essential for pre-determining the enzymatic digestibility of a cellulose sample.

Modifying cellulose structure could be a useful way to enhance the accessibility of cellulose for enzymatic hydrolysis (Weimer et al. 1991). Treatments with strong alkali or primary amines caused both delignification and conversion of native cellulose I to other forms. This results in the formation of different crystalline cellulose allomorphs that have different unit cell dimensions, chain packing schemes and hydrogen bonding relationships (Lokhande et al. 1977; Nishimura and Sarko 1987; Isogai and Atalla 1998; Langan et al. 2001; Wada et al. 2004). To date, six crystalline cellulose allomorphs (I, II, III_I, III_{II}, IV_I, IV_{II}) have been identified by their characteristic X-ray diffraction (XRD) patterns and solid-state ^{13}C nuclear magnetic resonance spectra.

Numerous studies in recent decades involving cellulase on cellulose have revealed the mechanisms by which the enzyme degrades cellulose (Sulzenbacher et al. 1997; Divne et al. 1998; Cao and Tan 2002). Different types of cellulases changed the DP, the solubility in aqueous alkali and cystallinity after hydrolysis (Reese et al. 1957; Sasaki et al. 1979; Puri 1984). Cellobiose yield was increased by using non-continuous hydrolysis process without further addition of enzyme (Vandergherm et al. 2010), while treated cellulose samples with alkali or anhydrous liquid ammonia affected enzyme digestibility based on the relative crystallinities (Mittal et al. 2011).

In the present work, the behavior of various crystalline celluloses allomorphs is examined and their effects were compared. There are only a few studies on the effects of polymorphy on hydrolysis of cellulose by enzymes. However, they focussed on either one or a few allomorphs, explored their kinetics, studied their molecular simulations and used bacteria for their treatment (Weimer et al. 1991; Wada et al. 2010; Beckham et al. 2011; Mittal et al. 2011). To the best of the authors' knowledge, no reports are yet available that compares enzymatic hydrolysis behavior of various crystalline celluloses with retention of constant DP. Therefore, in this study, hydrolysis behavior of the various crystalline celluloses during treatment by cellulase of *Trichoderma viride* is investigated.

Materials and Methods

Various crystalline cellulose and enzyme

Cotton linters (Buckeye 1AY-500) were used to prepare various crystalline cellulose samples according to the previous study (Abdullah et al. 2013). Briefly, cotton linters in their native state have the cellulose I (cell I) structure. Cellulose II (cell II) was prepared by mercerization using aqueous NaOH. Celluloses III_I (cell III_I) and III_{II} (cell III_{II}) were acquired from cell I and cell II, respectively, by using ethylenediamine treatment, while celluloses IV_I (cell IV_I) and IV_{II} (cell IV_{II}) were obtained from the prepared cell III_I and cell III_{II} samples by using glycerol treatment at 260 ˚C/0.6 MPa for 30 min.

The prepared samples of group I (celI I, cell III_I, cell IV_I) and group II (cell II, cell III_{II}, cell IV_{II}) celluloses were then adjusted by trial and error to give a common degree of polymerization (DP) by changing the treatment conditions mentioned above for converting cell I to various forms of celluloses. All these samples were found to contain similar components of 99.9 wt% glucose and 0.1 wt% xylose (TAPPI 1988).

The cellulase in lyophilized powder from *Trichoderma viride* Sigma C9422 was purchased from Nacalai Tesque, Japan. The activity of the enzymes was expressed in international units (U), i.e., one international unit of enzyme is defined as the amount that catalyzes the formation of one μmol of product per min under the defined conditions. The activity was found to be 11.4 U/ml.

Enzymatic hydrolysis of cellulose

In a 20 ml glass vials were added 35 mg/ml cellulose, 0.35 U/mg cellulose of cellulase and 0.05 M sodium acetate buffer of pH 5.0 (thermostated before at 50˚C) until 3 ml final volume. The pH value was adjusted using 1 M hydrochloric acid (HCl), if necessary (Bommarius et al. 2008). The controls together with the reaction mixtures were placed in an incubator at 50 ˚C and continuously stirred using magnetic stirrers. No β-glucosidase supplement was used in this study (Kadam et al. 2004). At the designated treatment times, the samples were removed and the enzyme reactions were terminated by quenching in ice bath, followed by centrifugation at 8000 × *g* for 2 min. The supernatant was immediately filtered, then refrigerated until subjected to analysis (Wyk 1997; Bommarius et al. 2008; Yang 2010).

Analyses of cellulose residue

Degree of polymerization (DP) – The molecular weight distribution of various celluloses was evaluated using phenyl carbamate derivatives. The procedure was modified from previously published methods (Evans et al. 1989, Mormann and Michel 2002). Cellulose (5 mg) and phenyl isocyanate (0.2 mL) were added to pyridine (2 mL), and its mixture was heated up to 80 ˚C under continuous stirring for 24 h to become a yellow transparent solution. Methanol (0.5 mL) was then added to terminate the reaction, and the solvent was removed by evaporation in vacuum to give dark yellow syrup.

The syrups of the phenyl carbamate derivatives were dissolved in tetrahydrofuran (THF). The solutions were then filtered through 0.45 μm microcentrifuge membrane filters prior to analysis by gel permeation chromatography (GPC) Shimadzu LC-10A under the following chromatographic conditions: column, Shodex

LF-804; column temperature, 40 ˚C; eluent, HPLC grade THF; flow-rate, 1.0 ml/min and detector, UV_{254nm}. Polystyrene standards were used to calibrate retention time for its molecular weight. The DP of cellulose was then calculated by dividing the molecular weights of the carbanilated cellulose by that of its repeating unit (=519) with the degree of substitution of 3.0. All reported values were based on the average of duplicate samples.

Crystallinity – The crystallinity was evaluated by using the X-ray diffraction (XRD) patterns that were recorded by X-ray diffractometer Rigaku RINT 2200 equipped with monochrometer. X-ray diffraction was conducted on reflectance modes through $7.5^\circ \leq 2\theta \leq 32.5^\circ$ by Cu-K_α radiation, operated at 40 kV and 30 mA. The cellulose sample was placed on a glass sample holder and flattened carefully, then mounted on the sample holder. Cellulose crystallinity was measured by deconvolution method as previously reported (Park et al. 2010). The XRD patterns were also simulated by using Mercury program according to the previous reports (French 2013; French and Cintrón 2013, Abdullah et al. 2013) and the crystallinity was then calculated as above. The crystallite size can be estimated according to its peak width at half maximum (pwhm) intensity by using Scherrer Eq. (1) (French and Cintrón 2013).

$$\tau = K\lambda / (\beta \cos\theta) \qquad (1)$$

In Eq. (1), τ is the crystallite size, K is a constant depends on the crystal shapes, λ is the wavelength of Cu-K_α =1.542 Å, β is the pwhm in radians and θ is the diffraction angle. The value of the variable crystal shape factor K is unknown, thus, it is assumed as K=1

The decomposition rate of the cellulose allomorphs was in addition estimated using a typical curve-fitting program, Origin.

Analysis of supernatant

Total sugars production - The total hydrolyzed products, cellobiose and glucose, in supernatant for each hydrolysis time points were measured by high performance liquid chromatography (HPLC) system Shidmadzu, LC-10A. The chromatographic conditions were: column, Bio-Rad Aminex HPX-87P x 7.8 mm; detector, UV_{254nm}; eluent, deionized water; flow-rate, 0.6 ml/min and oven temperature, 85 ˚C. The sample injection volume was 10 µl and the running time was 30 min.

Results and Discussion

Evaluation of cellulose residues

The main aim of this experiment was to investigate the behaviors of various crystalline celluloses in enzymatic hydrolysis as the treatment medium. For this purpose, it is essential that the starting materials have similar DPs in order to evaluate and compare directly their hydrolysis behaviors. As a result, the adjusted DP by trial and error and the corresponding crystallinity of the celluloses are summarized in Table 1. The XRD patterns of these celluloses are illustrated in Fig. 1.

Each of these celluloses was then treated with cellulase at pH 5.0 and 50 ˚C with solid concentration set to 35 mg/ml and enzyme loading of 0.35 U/mg cellulose. As the substrate is pure cellulose, higher loading of enzyme is unnecessary. The residue weights over times of the various celluloses after enzymatic hydrolysis are

presented in Fig. 2. During the 17 day hydrolysis treatment, the residue weights from these various celluloses are decreasing, with the highest rate during the first week. In group I, cell III_I hydrolyzed the most, and it has lesser residue than that of cell I and cell IV_I, which behave quite similarly. On the other hand, all celluloses in group II reach more or less similar yields and are seemingly equivalent to those of cell III_I. Generally, group II celluloses are easier to hydrolyze than those of group I, except for cell III_I.

The rate of decomposition of the cellulose allomorphs was also estimated using Origin program and it was found that the rate of decomposition for cell I, cell III_I and cell IV_I are 0.19, 0.49 and 0.21 wt% per day, respectively. While for group II celluloses, cell II, cell III_{II}, cell IV_{II} decomposed at 0.23, 0.24 and 0.30 wt% per day, respectively. From these estimations, it can be said that group I celluloses degraded slower than group II celluloses, except cell III_I.

Figure 3 shows the XRD patterns of group I celluloses after enzymatic hydrolysis. In Fig. 3 (*left*), residues from cell I remain almost unchanged even after 17 days hydrolysis treatment. However, the intensity at $2\theta \approx 22.5^\circ$ is decreasing as enzymatic hydrolysis is prolonged, and the peaks at $2\theta \approx 14.4^\circ$ and 16.3° are not sharp as observed in the control. This is seen in the progressive decrease in crystallinity in Fig. 6 (below) and may be due to the enzymatic attacks on the structure of the cell I (Lee et al. 1983; Cao and Tan 2005).

In Fig.3 (*middle*), the XRD patterns of residues from cell III_I demonstrate that the cell III_I is slowly converted back to cell I. Yet, the full XRD pattern of cell I is not obtained. During the treatment, the residues from cell III_I are observed to be gradually modified to a mixture of cell I and cell III_I. As for residues from cell IV_I, in Fig. 3 (*right*), no significant changes are observed, except for the peak at $2\theta \approx 15.1^\circ$. In both cases, some enzymatic attack could also have taken place.

Figure 4 shows the XRD patterns of group II celluloses after enzymatic hydrolysis. Though there is no significant change observed for the XRD patterns of cell II in Fig 4 (*left*), the intensity at $2\theta \approx 19.7^\circ$ and 22.0° decreases as enzymatic treatment time is prolonged. The XRD patterns of residues from cell III_{II} in Fig. 4 (*middle*) and cell IV_{II} in Fig. 4 (*right*), were slowly converted into their parent, cell II.

For cell III_{II} in Fig. 4 (*middle*), two peaks at $2\theta \approx 20.1^\circ$ and 21.6° emerge during the time of hydrolysis, comparable to the control, cell II. In contrast with Fig. 4 (*right*), the peak at $2\theta \approx 15.1^\circ$ for cell IV_{II} disappears after a few days' treatment, replicating the control cell II. Thus, from cell III_{II} in Fig. 4 (*middle*) and cell IV_{II} in Fig. 4 (*right*), mixtures comprising cell III_{II} and cell II, also cell IV_{II} and cell II, are present during the treatments. These behaviors of cellulose residues from cell III_I in Fig. 3 (*middle*); cell IV_I, in Fig. 3 (*right*); cell III_{II}, in Fig. 4 (*middle*) and cell IV_{II}, in Fig. 4 (*right*) were also examined under wet conditions by X-ray diffractometry with similar results.

Figure 5 shows XRD patterns of residues from cell III_I treated *with* and *without* enzyme. In these data, the changes from cell III_I into cell I occur *with* or *without* cellulase. However, the peaks at $2\theta \approx 14.4^\circ$ and 16.3° appear at a much slower rate *with* enzyme. Somehow, the enzymatic attacks must interfere with the conversion process. According to the literature, immersion of cell III_I in a polar solvent could result in cell III_I or cell I (Loeb and Segal 1955; Wada et al. 2008). Similar conversion of the crystalline form to its parent cellulose is also detectable with cell IV_I, cell III_{II} and cell IV_{II}, but is insignificant for cell IV_I, when it is treated *without* enzyme.

The simulation on XRD patterns based on previous studies (French 2013; French and Cintrón 2013, Abdullah et al. 2013), was done for all cellulose polymorphs. The simulated patterns (not shown) obtained at the

input pwhm seemed to match the experimental patterns (control celluloses) of both group I and group II celluloses. Thus, Table 2 summarizes the crystallite size and crystallinity of various celluloses at the corresponding input pwhm. The crystallite size and crystallinity of celluloses in group I is, respectively, seen to be similar to and higher than that in group II celluloses.

The simulated patterns demonstrated similar crystallinity as in the experimental patterns. Since there was no amorphous contribution to the Mercury simulation patterns, the amorphous part must have come from the deconvolution method, which could be the consequences of assumptions used. Such assumptions are built into the deconvolution routines, for examples: only the main peaks included in the deconvolution, the peak shape used being Gaussian instead of pseudo-Voigt (as assumed in the Mercury) etc.

Figure 6 shows the relationship between DP and crystallinity the celluloses after enzymatic hydrolysis. The crystallinity is observed to drop slowly after 1 day of treatment and then starts to decrease faster. The enzyme could probably attack first the amorphous regions of the celluloses, hence the crystallinity dropped slower at first, and then later would attack the crystalline parts. As for the DP, it is observed to decrease with treatment time. With cellulose in the modified forms (cell III_I, cell IV_I, cell II, cell III_{II}, cell IV_{II}), enzymatic hydrolysis reaction is shown to be more effective, compared with the cellulose in the cell I form. This agrees with previous work by Igarashi et al. (2007). This figure shows more changes occurred with group II than group I celluloses, and the changes during hydrolysis reaction were closely related to the initial cellulose structure.

The relationship of DP and hydrolyzed cellulose of various celluloses after enzymatic hydrolysis is illustrated in Fig. 7. More cellulose is hydrolyzed as the enzymatic hydrolysis is prolonged and the DP is decreased, similar with the observation of Fig. 6.

Evaluation of supernatant

The analysis of supernatant shows that enzymatic hydrolysis produces hydrolyzed products (total sugar) such as cellobiose and glucose. On average, more than 75 wt% of the total sugar consists of glucose. The results on total sugar obtained for various celluloses after enzymatic hydrolysis are shown in Fig. 8. Overall, cell III_I and group II celluloses produced similar total sugar yields, higher than those of cell I and cell IV_I. This confirms earlier findings that hydrolysis yield rates of cellulose III_I were much higher than for cellulose I (Igarashi et al. 2007), but for a more complete range of polymorphs and controlled DP.

Moreover, in this work, comparable yields of total sugar are obtainable from enzymatic hydrolysis of cell II and cell III_I, disagreeing with the previous work in which similar DPs were not considered for the starting materials (Mittal et al. 2011). The comparable behavior of cell I and cell IV_I could be because of the structures of cell IV_I and cell I are so similar (Wada et al. 2004).

The behaviors of various crystalline celluloses are seen to depend on the initial hydrolysis reactions. Given that the interconversion processes for some celluloses are most probably independent of the enzyme reaction, thus, the trends of total sugar productions are most likely due to intrinsic properties of the starting materials.

Concluding Remarks

In order to enhance enzymatic hydrolysis sugar production, various forms of crystalline celluloses were used as the starting materials. The modification of cellulose crystalline structures somehow assists the enzyme to perform better during hydrolysis reaction, although interconversion processes of the celluloses have taken place. In addition, considering constant DP for starting materials was necessary to improve the evaluation of enzymatic treatment of the various cellulose forms. From the results above, it is concluded that enzymatic hydrolysis treatment is better for cell III_I and group II celluloses, compared to native cellulose. Thus a recommendation can be made to either convert cell I into cell III_I or group II celluloses for enzymatic hydrolysis.

Acknowledgement

The authors are thankful for the support that was given by the Kyoto University Global GCOE program of 'Energy Science in the Age of Global Warming', for the completion of this work.

References

Abdullah R, Ueda K, Saka S (2013) Decomposition behaviors of various crystalline celluloses as treated by semi-flow hot-compressed water. Cellulose 20:2321-2333

Andersson S, Serimaa R, Paakkari T, Saranpää P, Pesonen E (2003) Crystallinity of wood and the size of cellulose crystallites in Norway spruce (Picea abies). J. Wood Sci. 49:531-537

Beckham GT, Matthews JF, Peters B, Bomble YJ, Himmel ME, Crowley MF (2011) Molecular-level origins of biomass recalcitrance: Decrystallization free energies for four common cellulose polymorphs. J. Phys. Chem. B 115:4118-4127

Bommarius A, Katona A, Cheben SE, Patel AS, Ragauskas AJ, Knudson K, Pu Y (2008) Cellulase kinetics as a function of cellulose pretreatment. Metab. Eng. 10:370-381

Cao Y, Tan H (2002) Effects of cellulase on the modification of cellulose. Carbohydr. Res. 337:1291–1296

Cao Y, Tan H (2005) Study on crystal structures of enzyme-hydrolyzed cellulosic materials by X-ray diffraction. Enzyme Microb. Technol. 36:314–317

Divne C, Ståhlberg J, Teeri TT, Jones TA (1998) High-resolution crystal structures reveal how a cellulose chain is bound in the 50 Å long tunnel of cellobiohydrolase I from Trichoderma reesei. J. Mol. Biol. 275:309-325

Evans R, Wearne RH, Adrian FA (1989) Molecular weight distribution of cellulose as its tricarbanilate by high performance size exclusion chromatography. J. Appl. Polym. Sci. 37:3291-3303

Fan LT, Lee YH, Beardmore DH (1980) Mechanism of the enzymatic hydrolysis of cellulose: effect of major structural features of cellulose on enzymatic hydrolysis. Biotechnol. Bioeng. 23:177-199

French AD (2014) Idealized powder diffraction patterns for cellulose polymorphs. Cellulose 21:885-896

French AD and Cintrón MS (2013). Cellulose polymorphy, crystallite size, and the Segal crystallinity index. Cellulose 20:583–588

Hall M, Bansal P, Lee JH, Realff MJ, Bommarius AS (2010) Cellulose crystallinity – a key predictor of the enzymatic hydrolysis rate. J. FEBS 277:1571-1582

Hsu T-A (1996) Pretreatment of biomass. In: Wyman CE (ed) Handbook on bioethanol: production and utilization. Taylor and Francis, Bristol, pp179-195

Igarashi K, Wada M, Hori R, Samejima M (2006) Surface density of cellobiohydrolase on crystalline celluloses – a critical parameter to evaluate enzymatic kinetics at a solid-liquid interface. FEBS J. 273:2869-2878

Igarashi K, Wada M, Samejima M (2007) Activation of crystalline cellulose to cellulose III_I results in efficient hydrolysis by cellobiohydrolase. FEBS J. 274:1785-1792

Isogai A, Atalla RH (1998) Dissolution of cellulose in aqueous NaOH solutions. Cellulose 5:309-319

Kadam KL, Rydholm EC, McMillan JD (2004) Development and validation of a kinetic model for enzymatic saccharification of lignocellulosic. Biotechnol. Progr. 20:698-705

Kumar S, Gupta R, Lee YY, Gupta RB (2010) Cellulose pretreatment in subcritical water: Effect of temperature on molecular structure and enzymatic reactivity. Bioresour. Technol. 101:1337–1347

Langan P, Nishiyama Y, Chanzy H (2001) X-ray Structure of mercerized cellulose II at 1 Å resolution. Biomacromolecules 2:410-416

Lee SB, Kim IH, Ryu DDY, Taguchi H (1983) Structural properties of cellulose and cellulase reaction mechanism. Biotechnol. Bioeng. 25:33-51

318 Loeb L, Segal L (1955) Studies of the ethylenediamine-cellulose complex. I. Decomposition of the complex by
319 solvents. J. Polym. Sci. 15:343-354
320 Lokhande HT, Shukla SR, Chidambareswaran PK, Patil NB (1977) Ethylenediamine-induced conversion of
321 cellulose I to cellulose III. J. Polym. Sci. Polym. Lett. Ed. 15:97-99
322 Mormann W, Michel U (2002) Improved synthesis of cellulose carbamates without by-products. Carbohydr.
323 Polym. 50:201-208
324 Mittal A, Katahira R, Himmel ME, Johnson DK (2011) Effects of alkaline or liquid-ammonia treatment on
325 crystalline cellulose: changes in crystalline structure and effects on enzymatic digestibility. Biotechnol.
326 Biofuels 4/41:1-16
327 Nishimura H, Sarko A (1987) Mercerization of cellulose. IV. Mechanism of mercerization and crystallite sizes.
328 J. Appl. Polym. Sci. 33:867-874
329 O'Sullivan AC (1997) Cellulose: the structure slowly unravels. Cellulose 4:173–207
330 Park S, Baker JO, Himmel ME, Parilla PA, Johnson DK (2010) Cellulose crystallinity index: measurement
331 techniques and their impact on interpreting cellulase performance. Biotechnol. Biofuels 3/10:1-10
332 Puri VP (1984) Effect of crystallinity and degree of polymerization of cellulose on enzymatic saccharification.
333 Biotechnol. Bioeng. 26:1219-1222
334 Reese ET, Segal L, Tripp VW (1957) The effect of cellulose on the degree of polymerization of cellulose and
335 hydrocellulose. Text. Res. J. 27:626-632
336 Sasaki T, Tanaka T, Nanbu N, Sato Y, Kainuma K (1979) Correlation between X-ray diffraction measurements
337 of cellulose crystalline structure and the susceptibility to microbial cellulose. Biotechnol. Bioeng. 21:1031-
338 1042
339 Schacht C, Zetzl C, Brunner G (2008) From plant materials to ethanol by means of supercritical fluid
340 technology. J Supercrit. Fluids 46:299–321
341 Sulzenbacher G, Schülein M, Davies GJ (1997) Structure of the endoglucanase I from Fusarium oxysporum:
342 native, cellobiose, and 3,4-epoxybutyl β-D-cellobioside-inhibited forms, at 2.3 Å resolution. Biochemistry
343 36:5902-5911
344 TAPPI Standard Methods T222 om-88 (1988)
345 Vanderghem C, Boquel P, Blecker C, Paquot M (2010) A multistage process to enhance cellobiose production
346 from cellulosic materials. Appl. Biochem. Biotechnol. 160:2300-2307
347 Wada M, Chanzy H, Nishiyama Y, Langan P (2004) Cellulose III_I crystal structure and hydrogen bonding by
348 synchrotron X-ray and neutron fiber diffraction. Macromolecules 37:8548-8555
349 Wada M, Kwon GJ, Nishiyama Y (2008) Structure and thermal behavior of a cellulose I-ethylenediamine
350 complex. Biomacromolecules 9:2898-2904
351 Wada M, Ike M, Tokuyasu K (2010) Enzymatic hydrolysis of cellulose I is greatly accelerated via its conversion
352 to the cellulose II hydrate form. Polym. Degrad. Stab. 95:543-548
353 Ward RJ (2011) Cellulase engineering for biomass saccharification. In: Buckeridge MS, Goldman GH (eds)
354 Routes to cellulosic ethanol. Springer, New York, pp135-151
355 Weimer PJ, French AD, Calamari TA Jr (1991) Differential fermentation of cellulose allomorphs by ruminal
356 cellulolytic bacteria. Appl. Environ. Microbiol. 57:3101-3106

Wyk JPHV (1997) Cellulose hydrolysis and cellulase adsorption after pretreatment of cellulose materials. Biotechnol. Tech. 11:443-335

Yang J, Zhang X, Yong Q, Yu S (2010) Three-stage hydrolysis to enhance enzymatic saccharifcation of steam-exploded corn stover. Bioresour. Technol. 101:4930-4935

Yoshida M, Liu Y, Uchida S, Kawarada K, Ukagami Y, Ichinose H, Kaneko S, Fukuda K (2008) Effects of cellulose crystallinity, hemicellulose, and lignin on the enzymatic hydrolysis of *Miscanthus sinensis* to monosaccharides. Biosci. Biotechnol. Biochem. 72:805-810

List of figure captions

Fig. 1 The XRD patterns of various crystalline celluloses prepared in this study

Fig. 2 The residues obtained from various crystalline celluloses after enzymatic hydrolysis

Fig. 3 The XRD patterns of group I celluloses; cell I (*left*), cell III_I (*middle*), cell IV_I (*right*), after enzymatic hydrolysis

Fig. 4 The XRD patterns for group II celluloses; cell II (*left*), cell III_{II} (*middle*), cell IV_{II} (*right*), after enzymatic hydrolysis

Fig. 5 The comparison between XRD patterns of residues from cell III_I when treated *with* and *without* enzyme

Fig. 6 The changes in DP and crystallinity of various crystalline cellulose after enzymatic hydrolysis

Fig. 7 The changes in DP and hydrolyzed cellulose of various crystalline celluloses after enzymatic hydrolysis

Fig. 8 The yield of total sugars from various crystalline celluloses after enzymatic hydrolysis

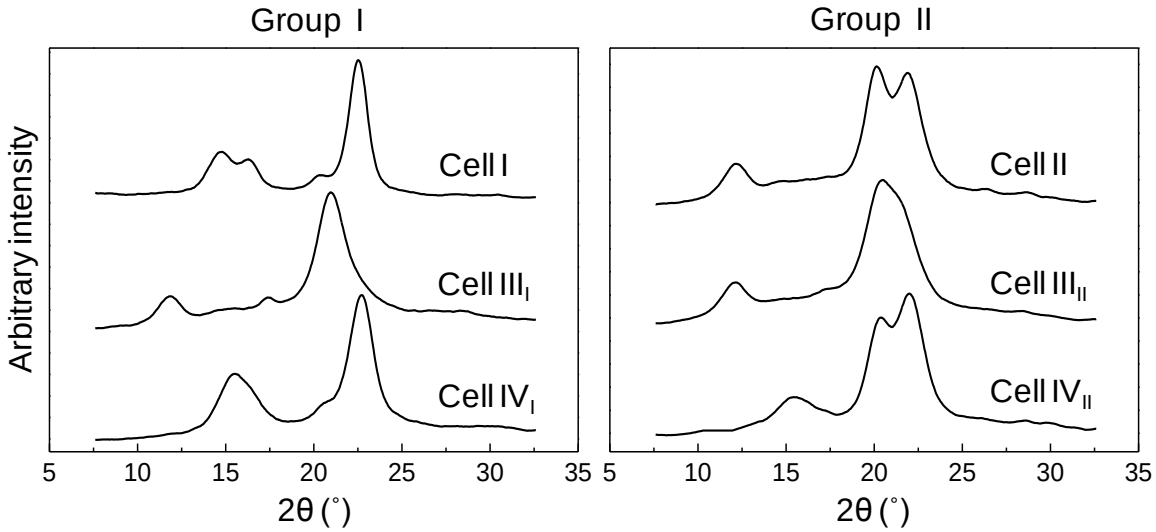

Fig. 1 The XRD patterns of various crystalline celluloses prepared in this study

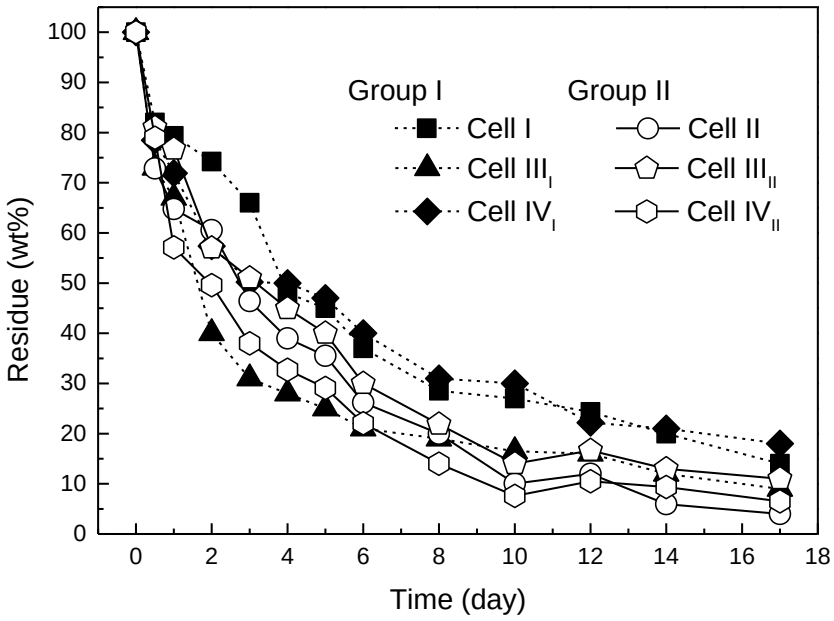

Fig. 2 The residues obtained from various crystalline celluloses after enzymatic hydrolysis

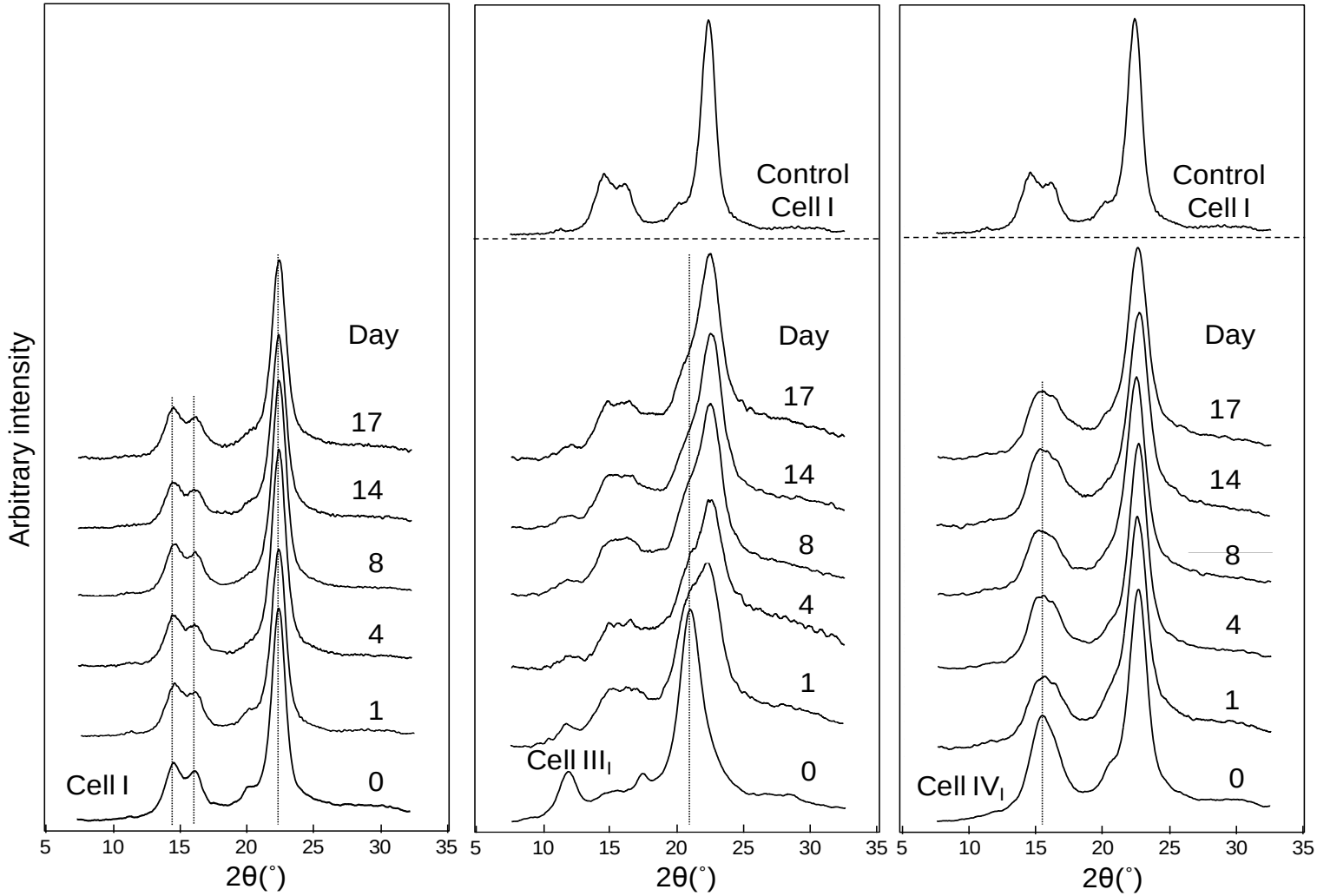

Fig. 3 The XRD patterns of group I celluloses; cell I (*left*), cell III_I (*middle*), cell IV_I (*right*), after enzymatic hydrolysis

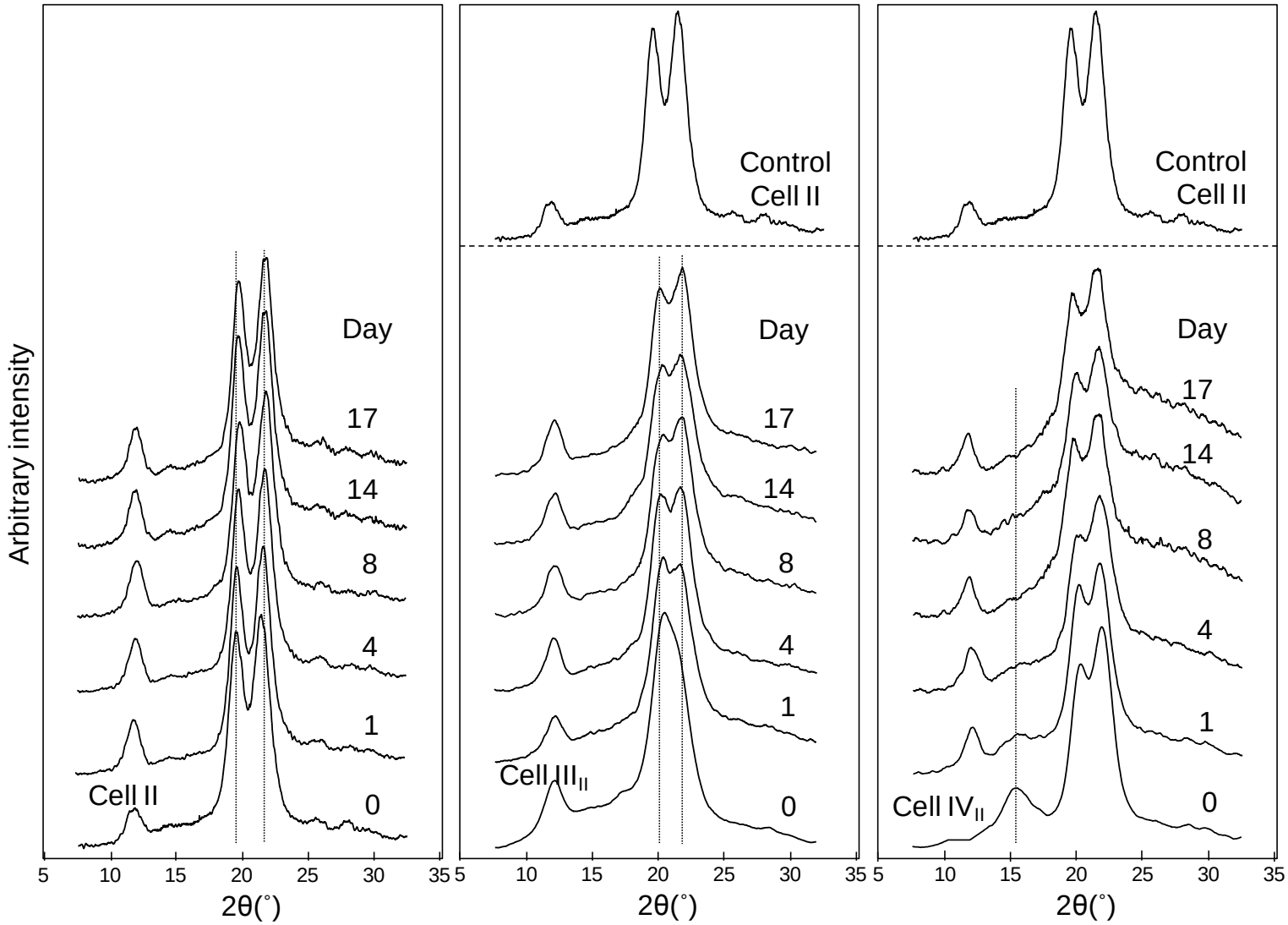

Fig. 4 The XRD patterns for group II celluloses; cell II (*left*), cell III$_{II}$ (*middle*), cell IV$_{II}$ (*right*), after enzymatic hydrolysis

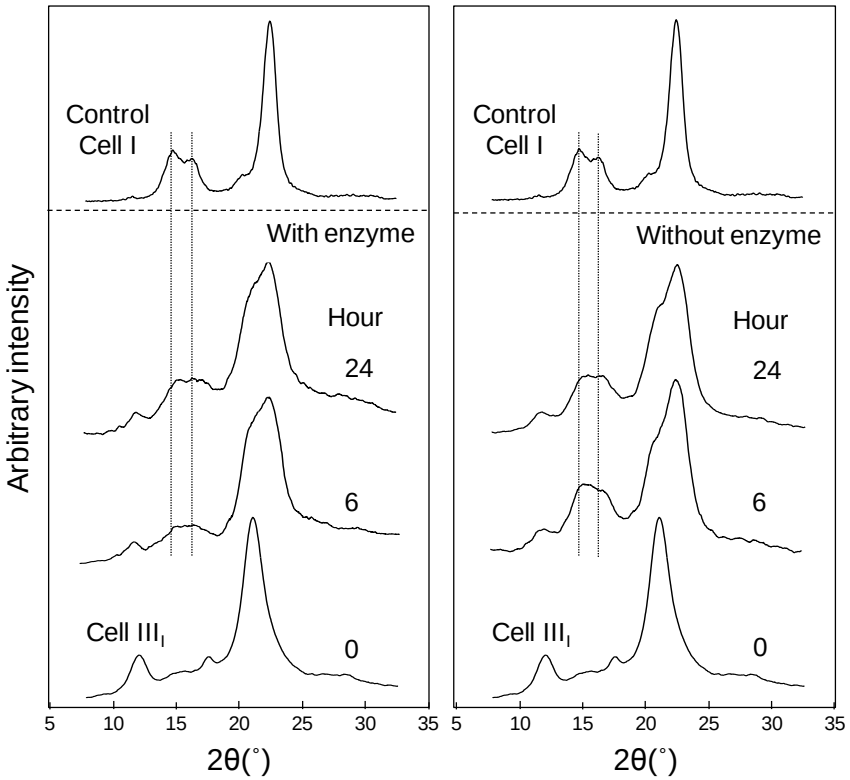

Fig. 5 The comparison between XRD patterns of residues from cell III_I when treated *with* and *without* enzyme

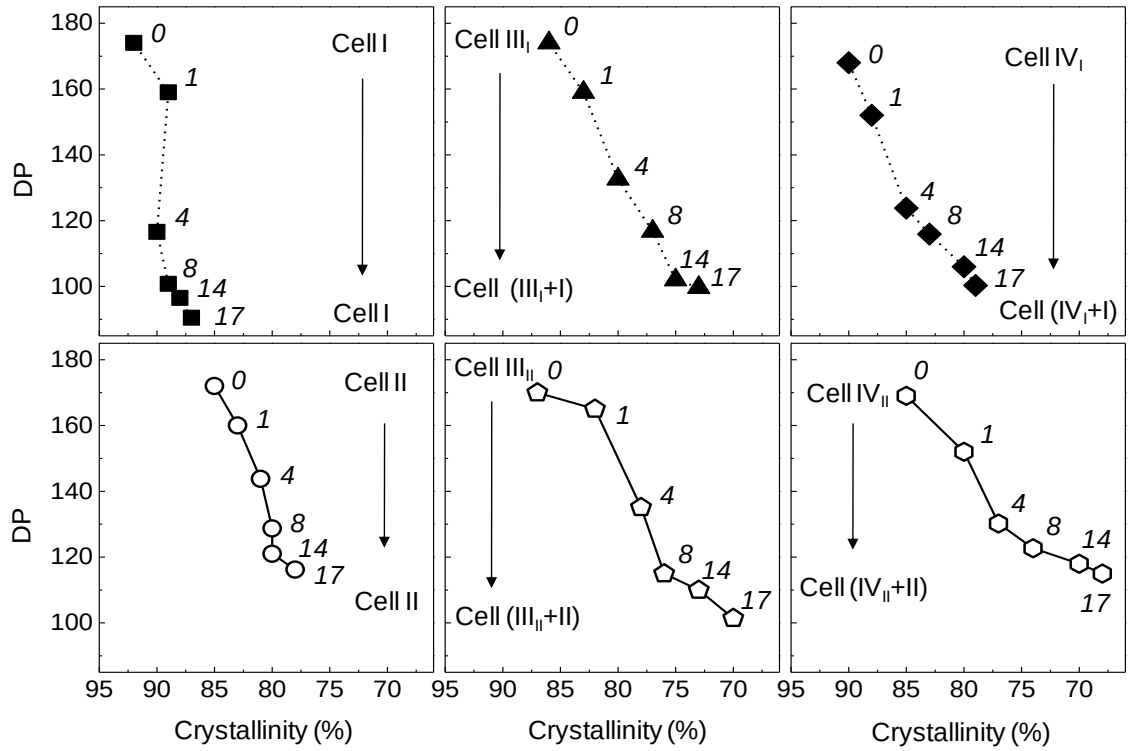

Fig. 6 The changes in DP and crystallinity of various crystalline cellulose after enzymatic hydrolysis

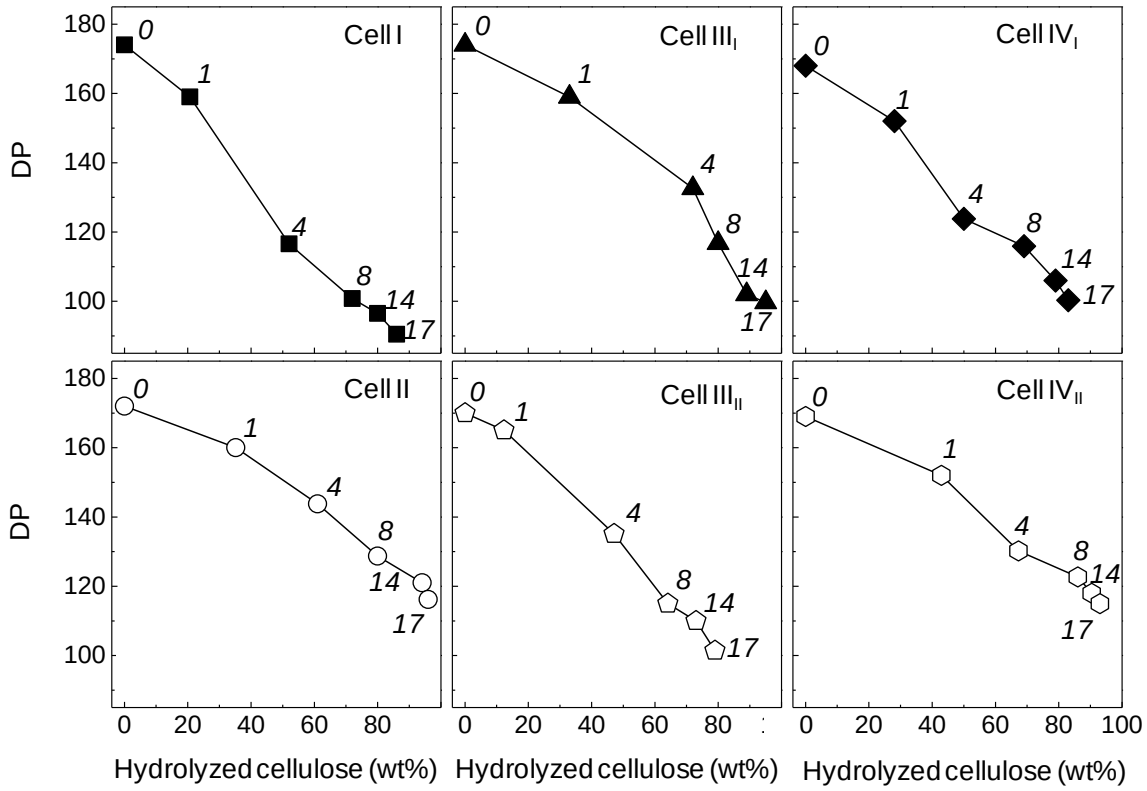

Fig. 7 The changes in DP and hydrolyzed cellulose of various crystalline celluloses after enzymatic hydrolysis

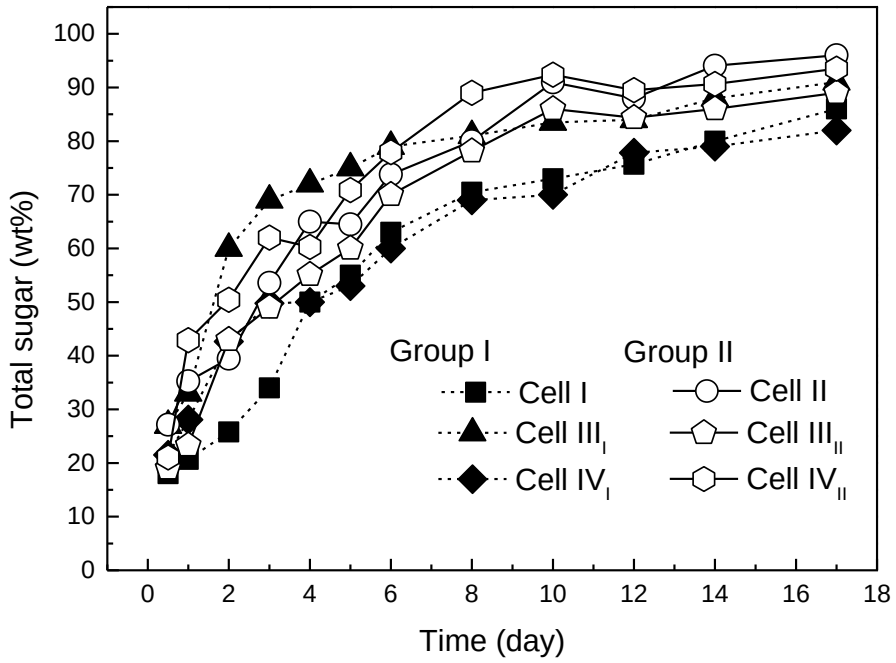

Fig. 8 The yield of total sugars from various crystalline celluloses after enzymatic hydrolysis

Table 1 The DP and crystallinity of various crystalline celluloses as starting materials

	Cell	DP	Crystallinity (%)
Group I	I	174	91.8
	III_I	174	86.0
	IV_I	168	89.6
Group II	II	172	85.3
	III_{II}	170	87.2
	IV_{II}	169	85.0

Table 2 The pwhm, crystallite size and crystallinity of the simulated various celluloses

	Cell	Input pwhm (˚)[a]	τ, crystallite size (Å)[b]	Crystallinity (%)
Group I	I	1.3	69.3	86.4
	III_I	2.5	35.9	89.7
	IV_I	1.8	50.0	90.1
Group II	II	1.8	49.8	83.5
	III_{II}	3.5	25.6	85.3
	IV_{II}	1.3	69.0	76.2

[a]Based on the simulated pattern that matches the experimental pattern (control cellulose)
[b]Estimated using Scherrer equation with K=1